frontiers in Marine Science

ORIGINAL RESEARCH
published: 27 March 2018
doi: 10.3389/fmars.2018.00105

Photochemical vs. Bacterial Control of H_2O_2 Concentration Across a pCO_2 Gradient Mesocosm Experiment in the Subtropical North Atlantic

Mark J. Hopwood[1]*, *Ulf Riebesell*[1], *Javier Arístegui*[2], *Andrea Ludwig*[1], *Eric P. Achterberg*[1] *and Nauzet Hernández*[2]

[1] GEOMAR Helmholtz Centre for Ocean Research Kiel, Kiel, Germany, [2] Instituto de Oceanografía y Cambio Global (IOCAG), Universidad de Las Palmas de Gran Canaria (ULPGC), Las Palmas, Spain

In the surface ocean, microorganisms are both a source of extracellular H_2O_2 and, via the production of H_2O_2 destroying enzymes, also one of the main H_2O_2 sinks. Within microbial communities, H_2O_2 sources and sinks may be unevenly distributed and thus microbial community structure could influence ambient extracellular H_2O_2 concentrations. Yet the biogeochemical cycling of H_2O_2 and other reactive oxygen species (ROS) is rarely investigated at the community level. Here, we present a time series of H_2O_2 concentrations during a 28-day mesocosm experiment where a pCO_2 gradient (400–1,450 μatm) was applied to subtropical North Atlantic waters. Pronounced changes in H_2O_2 concentration were observed over the duration of the experiment. Initially H_2O_2 concentrations in all mesocosms were strongly correlated with surface H_2O_2 concentrations in ambient seawaters outside the mesocosms which ranged from 20 to 92 nM over the experiment duration (Spearman Rank Coefficients 0.79–0.93, p-values < 0.001–0.015). After approximately 9 days of incubation however, H_2O_2 concentrations had increased across all mesocosms, later reaching >300 nM in some mesocosms (2–6 fold higher than ambient seawaters). The correlation with ambient H_2O_2 was then no longer significant ($p > 0.05$) in all treatments. Furthermore, changes in H_2O_2 could not be correlated with inter-day changes in integrated irradiance. Yet H_2O_2 concentrations in most mesocosms were inversely correlated with bacterial abundance (negative Spearman Rank Coefficients ranging 0.59–0.94, p-values < 0.001–0.03). Our results therefore suggest that ambient H_2O_2 concentration can be influenced by microbial community structure with shifts toward high bacterial abundance correlated with low extracellular H_2O_2 concentrations. We also infer that the nature of mesocosm experiment design, i.e., the enclosure of water within open containers at the ocean surface, can strongly influence extracellular H_2O_2 concentrations. This has potential chemical and biological implications during incubation experiments due to the role of H_2O_2 as both a stressor to microbial functioning and a reactive component involved in the cycling of numerous chemical species including, for example, trace metals and haloalkanes.

Keywords: hydrogen peroxide, H_2O_2, mesocosm, Atlantic, pCO_2

OPEN ACCESS

Edited by:
Jörg Wiedenmann, University of Southampton, United Kingdom

Reviewed by:
Marta Plavsic, Rudjer Boskovic Institute, Croatia
Bernhard Riegl, Nova Southeastern University, United States

***Correspondence:**
Mark J. Hopwood
mhopwood@geomar.de

Specialty section:
This article was submitted to Marine Biogeochemistry, a section of the journal Frontiers in Marine Science

Received: *25 July 2017*
Accepted: *14 March 2018*
Published: *27 March 2018*

Citation:
Hopwood MJ, Riebesell U, Arístegui J, Ludwig A, Achterberg EP and Hernández N (2018) Photochemical vs. Bacterial Control of H_2O_2 Concentration Across a pCO_2 Gradient Mesocosm Experiment in the Subtropical North Atlantic. Front. Mar. Sci. 5:105. doi: 10.3389/fmars.2018.00105

INTRODUCTION

Reactive oxygen species (ROS) are ubiquitous in sunlit natural surface waters (Van Baalen and Marler, 1966; Moore et al., 1993; Miller and Kester, 1994). The most extensively measured ROS in the marine environment, H_2O_2, is present in the surface mixed layer at concentrations on the order of 10–100 nM (Price et al., 1998; Yuan and Shiller, 2001; Gerringa et al., 2004). In the surface ocean, H_2O_2 is known to be mainly produced by photochemistry (Fujiwara et al., 1993; Micinski et al., 1993) with a poorly quantified fraction produced via biochemical processes (Palenik et al., 1987; Croot et al., 2005; Milne et al., 2009). Biochemical processes are also used to explain H_2O_2 production in the dark (Palenik and Morel, 1988; Moffett and Zafiriou, 1990; Vermilyea et al., 2010).

H_2O_2 can cross cell membranes and cause a wide range of cellular damage, a process generically referred to as oxidative stress (Seaver and Imlay, 2001; Lesser, 2006; Imlay, 2008). Extracellular H_2O_2 is however not generally considered to be a major constraint on cellular growth under natural conditions in the marine environment because most microorganisms are thought to produce catalase and peroxidase enzymes which control H_2O_2 decomposition rates in the surface ocean (Moffett and Zafiriou, 1990; Petasne and Zika, 1997). However, recent work has challenged the assumption that extracellular H_2O_2 at nanomolar concentrations does not negatively influence cellular metabolism in surface seawater. The susceptibility of a range of marine microorganisms to H_2O_2 (Bogosian et al., 2000; Morris et al., 2011) and measurable effects on primary metabolism at extracellular H_2O_2 concentrations within the range of surface marine concentrations (Morris et al., 2011; Baltar et al., 2013) have been demonstrated. Furthermore, it has been suggested that microbes sensitive to H_2O_2 may not be cultivable under normal laboratory conditions (Morris et al., 2008, 2011), which may have severely biased our historical understanding of ROS interactions with marine microorganisms.

H_2O_2 production rates, decomposition rates, and effects on cellular functioning may vary widely at the species level (Palenik et al., 1987; Baltar et al., 2013). Furthermore, cross-group interactions may be important in regulating ambient extracellular H_2O_2 concentrations (Morris et al., 2011). Investigations at the community level are therefore required in order to comprehensively understand the interaction between biological processes and ROS in seawater. Mesocosm studies are one approach by which this could be achieved, yet rapid decay rates mean that investigating ROS during an offshore mesocosm experiment, with a setup for example as per Taucher (2017, this Research Topic), would be logistically challenging. A mesocosm experiment on a smaller and more accessible scale, with a similar pCO_2 gradient and timespan, was therefore conducted in the subtropical waters of Gran Canaria in March 2016. Our objective was to compare changes in ROS and other short-lived reactive species over the timescale of an induced phytoplankton bloom across a broad pCO_2 gradient. The pCO_2 gradient was designed to encompass pCO_2 under all plausible future climate scenarios until 2100 (IPCC Working Group 1, 2014) with the addition of some higher end-members to investigate potential thresholds with respect to CO_2-sensitive ecological and biogeochemical processes.

MATERIALS AND METHODS

Mesocosm Design

The mesocosm study, conducted in Taliarte Harbor, Gran Canaria in March 2016, used eight thermoplastic polyurethane bags with a 2 m diameter, a depth of ∼3 m, a starting volume of ∼8,000 L, and no lid or screen on top. The bags were mounted on a buoyant frame which was allowed to drift ∼2–3 m away from a sampling jetty. After filling with ambient seawater (on 1 March, experiment day −4), pumped from outside Taliarte Harbor (depth 15 m), the mesocosms were allowed to function without nutrient addition for 21 days (**Supplementary Figure 1**). A pCO_2 gradient across the eight mesocosms was induced on day 0 by the addition of varying volumes of filtered, CO_2 saturated seawater using a custom made "spider" distribution device described by Riebesell et al. (2013). The pCO_2 gradient (400–1,450 μatm) was designed to be similar to that used during the offshore KOSMOS mesocosm experiment conducted in Gando Bay, Gran Canaria in September/October 2014 (Taucher, 2017, this Research Topic). A further top-up of pCO_2 saturated seawater was then made to the mesocosms as necessary to maintain the pCO_2 gradient (**Supplementary Figure 1**) following CO_2 outgassing. The precise volume of each mesocosm was determined (on day 18) by measuring salinity before, and after, the addition of 40 L freshwater to each mesocosm, similar to Czerny et al. (2013). A single macronutrient addition (3.1 μM nitrate, 1.5 μM silicate, and 0.2 μM phosphate) was then made (after day 18 sampling).

Analysis

H_2O_2 samples were collected in opaque 125 mL high density polyethylene (HDPE) bottles (Nalgene) which were pre-cleaned (1 day soak in detergent, 1 week soak in 1 M HCl, three rinses with de-ionized water; 18.2 MΩ·cm, Milli-Q, Millipore) and dried in a laminar flow hood prior to use. Sample bottles were rinsed once with seawater and filled with no headspace by gently submerging the bottles within the mesocosms. Chlorophyll a, bacterial abundance, chromophoric dissolved organic matter (CDOM) and macronutrient concentrations were determined from depth integrated water samples collected using 2.5 m long custom-made samplers with an internal volume of ∼10 L. These samplers were constructed from polypropylene tubing with valves at both ends. After filling, by submerging into the mesocosms and closing the valves, the samplers were removed and gently inverted to facilitate mixing. Samplers were then slowly drained through 1 cm diameter silicone tubing into pre-rinsed (de-ionized water and then mesocosm water) 25 L transparent HDPE containers, which were then transferred to shaded boxes and moved to a dark, refrigerated room for sub-sampling. Analysis of chlorophyll a and macronutrients then began immediately.

Chlorophyll a was measured by fluorometry as per Welschmeyer (1994) and macronutrient concentrations (nitrate + nitrite, phosphate, silicate) were determined by colorimetry as per Hansen and Koroleff (1999). CDOM absorption spectra

were measured with a 100 cm, 250 μL capillary (LPC100CM) connected via an optical fiber to a light source (DH2000BAC) and a USB2000+UV-VIS ES detector (Ocean Optics). The system was controlled using Spectra-suite software (Ocean Optics). Samples were injected into the capillary with a peristaltic pump at a flow rate of 1 mL min^{-1}. Relative molecular weight was estimated from CDOM absorption by deriving the slope ratio (S_R) as the ratio of the slope of the shorter wavelength region (275–295 nm) to that of the longer wavelength region (350–400 nm; Helms et al., 2008). The spectral slopes were calculated from the linear regression of the log-transformed absorption spectra.

H_2O_2 was always analyzed within 1 h of collection via flow injection analysis (FIA) using the Co(II) catalyzed oxidation of luminol (Yuan and Shiller, 1999). A FIA system was assembled and operated exactly as per Hopwood et al. (2017) resulting in a detection limit of <1 nM. Calibrations were run daily, and with every new reagent batch, by at least six standard additions of diluted H_2O_2 (TraceSelect, Fluka) to aged (stored at room temperature for >48 h) seawater (unfiltered). The stability of H_2O_2 stock solution was checked by measuring absorbance at 240 nm using a quartz 10 cm cell and a USB4000 spectrometer (Ocean Optics). H_2O_2 (TraceSelect, Fluka) was sequentially diluted weekly to create stock solutions of 100 mM and 100 μM using de-ionized water. With respect to the measurement of chemical species other than H_2O_2, the H_2O_2 luminol based FIA method is expected to be robust for measurements in oxygenated surface seawater (Yuan and Shiller, 1999, 2004).

Bacterial counts were obtained on depth integrated water samples. Two mL water samples were fixed with 1% paraformaldehyde (final concentration) and stored at −80°C until analysis. Samples were analyzed by flow cytometry (FACSCalibur, Becton Dickinson), with a 15 mW laser set to excite at 488 nm (Gasol and del Giorgio, 2000). Subsamples (400 μL) for the determination of heterotrophic bacteria were stained with the fluorochrome SybrGreen-I (4 μL) at room temperature for 20 min and run at a flow rate of 16 μL min^{-1}. Cells were enumerated in a bivariate plot of 90° light scatter and green fluorescence. Molecular Probes latex beads (1 μm) were used as internal standards.

Ancillary Measurements

A CTD cast (using a CTD60M, Sea and Sun Technology) was conducted every sample collection day in all mesocosms. Additionally, a CTD cast was conducted on the sampling jetty adjacent to the mesocosms where a H_2O_2 sample in ambient seawater was also collected alongside every mesocosm sampling event. Photosynthetically active radiation (PAR) data was obtained from an ELDONET (Häder and Lebert, 2006) monitoring site located <200 m from the mesocosm jetty. Complete diurnal light profiles were available for experiment day 7 onwards, excluding days 12 and 13.

The diurnal change in H_2O_2 concentration in ambient seawater, and inside two mesocosms, was monitored by setting up FIA equipment on the mesocosm sampling jetty with a PTFE sampling line weighted to float ∼10 cm below the water surface. Seawater was pumped continuously using a peristaltic pump (MiniPuls 3, Gilson) with a time delay between water inflow and analysis of ∼60–120 s. The sample line was used without a filter and visually inspected regularly for blockage. Calibration was undertaken three times in every 24 h period by 6–8 standard additions of H_2O_2 into aged (>48 h in the dark) seawater. A coiled 3 m PTFE sample line, which could be extended to the bottom of the mesocosms, was used to determine whether H_2O_2 was vertically homogenous within the mesocosm bags. During the diurnal experiment monitoring ambient seawater, salinity was measured regularly (<3 h intervals) using a LF 325 conductivity meter (WTW) which was calibrated before use with a KCl solution.

During rain events, rainwater was collected by deploying open low density polyethylene (LDPE) bags adjacent to the mesocosms. Rainwater was diluted prior to analysis by spiking 200 μL unfiltered rainwater into 50 mL aged seawater with the H_2O_2 concentration in seawater measured before, and after, the rainwater spike.

RESULTS

Mesocosm Time Series

Time series for the core parameters discussed herein are included in **Supplementary Datasheet 1**. Initial measurements in the mesocosms (2 March 2016, experiment day −3, after filling the mesocosms—but before any treatments were applied) verified that the enclosed waters were close to identical with respect to H_2O_2 concentration. Differences between the eight enclosures (range 38.3–40.9 nM, mean 39.3 ± 0.8 nM) were small compared to the detection limit of the analytical method (<1 nM; Croot et al., 2004; Hopwood et al., 2017) and the standard deviation of quadruple measurements of H_2O_2 in seawater collected on the sample jetty (mean 3.3 nM over the experiment duration). Depth profiles within a mesocosm bag (∼3 m depth) were conducted on day 25 mid-afternoon, when any stratification was expected to be maximal, and verified that H_2O_2 concentration was relatively well-mixed with only a slight vertical gradient (increasing from 43 to 51 nM bottom-top, mean 47 ± 3.5 nM). On day 12, surface seawater collected using a small inflatable boat showed a range of H_2O_2 concentrations at different locations around Taliarte Harbor (39 ± 9.9 nM, $n = 4$), outside the harbor within 150 m of the coastline (63 ± 1.8 nM, $n = 3$) and outside the harbor >400 m offshore (38 ± 5.6 nM, $n = 4$). Ambient seawater concentrations within the harbor (used to determine a background concentration for comparison with the mesocosms) were therefore similar to those found in near-shore waters.

The imposition of a large pCO_2 gradient across the mesocosm bags after sampling on day 0 had no clear prolonged effect on observed H_2O_2 concentrations (**Figure 1A**). Temporal trends in H_2O_2 concentration were relatively similar in all mesocosms until day 9 of the experiment with the standard deviation ranging from 0.7 to 13 nM. Data for mesocosm 1 are shown only until day 3, after which exchange with surrounding seawater occurred following leakage, and monitoring was thus discontinued. After day 9 the enclosed waters diverged and some mesocosms experienced swings to very high (>300 nM) H_2O_2 concentrations compared to ambient water (**Figure 1A**).

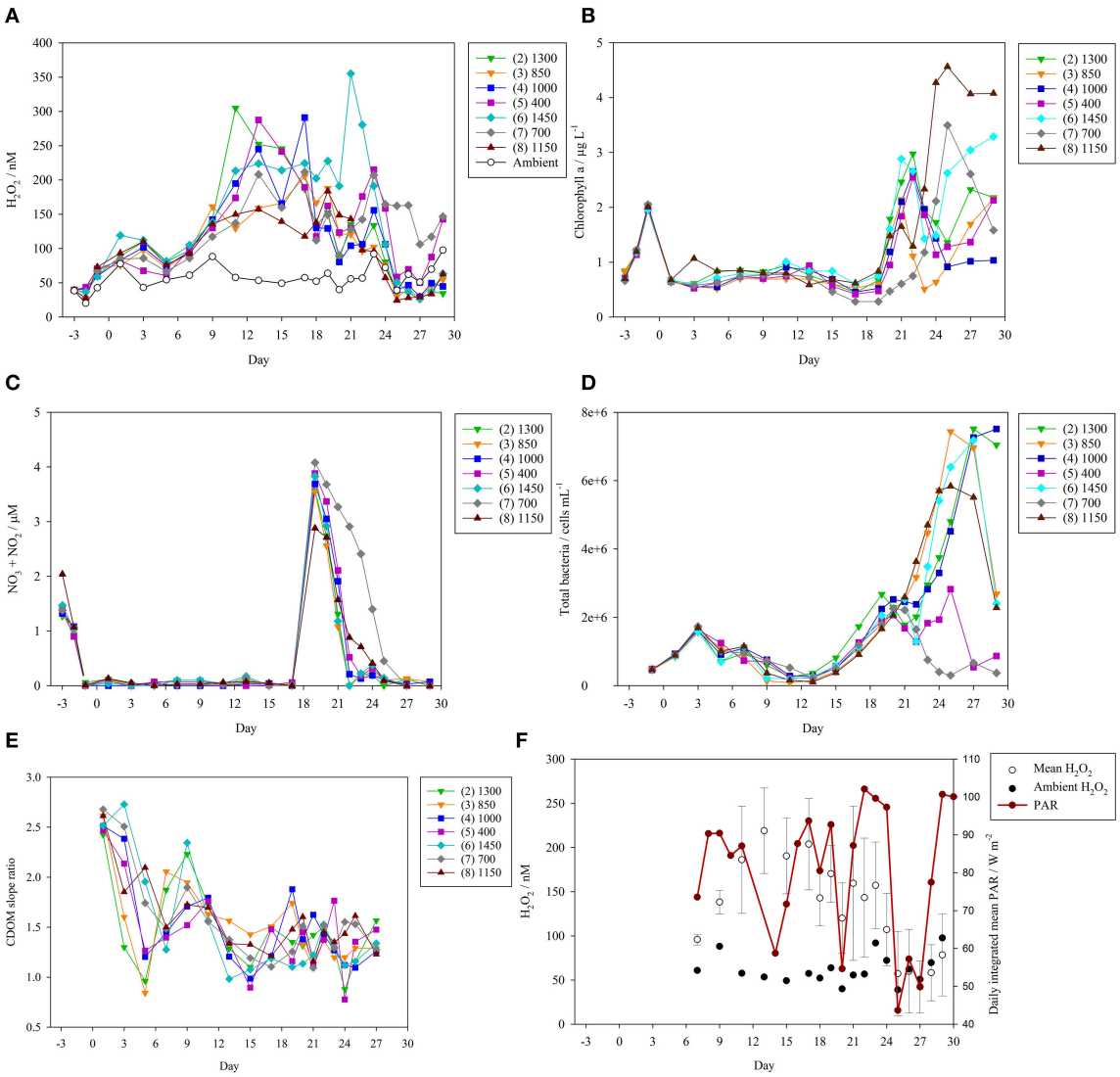

FIGURE 1 | Time series of core parameters over the experiment duration. The eight mesocosms (numbered 1–8) were subject to a pCO_2 gradient (400–1,450 µatm) imposed by the addition of CO_2 saturated, filtered seawater on day 0 (5 March 2016). Labels refer to target pCO_2 levels (µatm) which were obtained on pCO_2 addition days (see **Supplementary Figure 1**). The 550 µatm pCO_2 mesocosm (1) was discontinued after day 3 due to leakage and exchange with outside seawater and so no data is shown. **(A)** H_2O_2 concentrations (nM) during the mesocosm experiment. H_2O_2 concentration was also measured in ambient surface seawater outside the mesocosms (open circles). **(B)** Chlorophyll a concentrations (µg L^{-1}, depth integrated samples) throughout the experiment. **(C)** Nitrate + nitrite concentrations (µM, depth integrated samples) throughout the experiment. One macronutrient addition (3.1 µM nitrate, 1.5 µM silicate, and 0.2 µM phosphate) was made on day 18 to stimulate a phytoplankton bloom. **(D)** Total bacteria (cells mL^{-1}) during the mesocosm experiment. **(E)** Chromophoric dissolved organic matter (CDOM) slope ratio (S_R), a dimensionless parameter that is inversely proportional to molecular weight. **(F)** Photosynthetically active radiation (PAR, mean irradiance integrated over each experiment day, W m^{-2}), available only for experiment day 7 onwards, compared to ambient seawater and mean (±standard deviation) mesocosm H_2O_2 concentration.

Over the duration of the mesocosm experiment, ambient surface seawater H_2O_2 concentrations ranged from only 20–92 nM.

The initial nitrate concentration present in ambient seawater was depleted rapidly after filling of the mesocosms (**Figure 1C**). Nitrate + nitrite fell to <0.1 µM in all mesocosms by day −1. Nitrate concentration then remained depleted until the macronutrient addition on day 18 (macronutrient addition occurred after sampling on day 18). Correspondingly, a small peak in chlorophyll a was observed in all mesocosms on day −1 (**Figure 1B**). Chlorophyll a then declined to low concentrations until a larger peak following the macronutrient addition on day 18. Maximum chlorophyll a was then observed in most mesocosms on days 21–22.

A notable exception to the general trend in mesocosm H_2O_2 under post-bloom conditions was mesocosm 7 (700 µatm pCO_2). On days 25–27, H_2O_2 concentrations in the majority of mesocosms dropped below those measured in ambient

seawater, but H_2O_2 in mesocosm 7 always remained >100 nM (**Figure 1A**). Mesocosm 7 was also anomalous with respect to the bloom development. In mesocosm 7 only it appeared that grazing may have impeded bloom development after nutrient addition (this was consistent with higher meso-zooplankton abundances in mesocosm 7, data not shown), as evidenced by a noticeably slower decline in nitrate concentration (**Figure 1C**) and a late peak in chlorophyll a (**Figure 1B**).

Bacterial abundance was similar in all mesocosms until after nutrient addition (**Figure 1D**). Unlike chlorophyll a however, an increase in bacterial abundance was evident in all treatments prior to the nutrient addition on day 18. A small dip in bacterial abundance was then evident in most mesocosms between days 19 and 22. Under post-bloom conditions bacterial abundance was lowest in the anomalous treatment (700 µatm) and the 400 µatm pCO_2 mesocosm with notably elevated abundances in all pCO_2 enriched treatments. The observed trend in bacterial abundance can be interpreted as resulting from grazing pressure, and enhanced growth rates post-nutrient addition. Bacterial abundance pre-nutrient addition was inversely related to nanoeukaryotes' abundance due to grazing pressure. The increase in bacterial abundance from day 13 reflected a decline in the abundance of nanoeukaryotes. After nutrient addition (day 18), grazing on bacteria was probably considerable, but bacterial growth was enhanced sufficiently to overcome grazing pressure (except in the anomalous treatment). An in depth discussion of phytoplankton community structure over the experiment duration will be presented in a companion text.

The trend in CDOM over the experiment duration was similar across all pCO_2 treatments. The generally higher S_R at the start of the experiment (**Figure 1E**) corresponds to lower mean molecular weight and suggests an overall increase in CDOM molecular weight over the experiment duration. Photochemical bleaching would be expected to have had the opposite effect; to have produced low molecular weight CDOM from high molecular weight CDOM (i.e., to have increased S_R). Thus, the overall trend suggests that bacterial production of high molecular weight CDOM exceeded the rate of photochemical bleaching. Only between experiment days 7 and 13 was a sustained increase in S_R evident across most mesocosms and this corresponded to a temporary decline in bacterial abundance (**Figure 1D**).

Photosynthetically active radiation (PAR) data was available from day 7 until the end of the mesocosm experiment (**Figure 1F**) from a recording site close to the mesocosm jetty (<200 m displacement). Integrated daily PAR was subject to notable variations over the duration of the experiment ranging from a mean irradiance of 44 (day 25) to 102 (day 22) W m^{-2}.

Diurnal Cycling of H_2O_2

The diurnal cycling of H_2O_2 was followed both in ambient seawater (**Figure 2**) and inside mesocosm numbers 6 (1,450 µatm pCO_2, **Figure 3A**) and 5 (400 µatm pCO_2, **Figure 3B**) on days 22 and 23, respectively. Gaps in the data series corresponded to periods when standard additions were analyzed, the FIA instrument was cleaned, or malfunctions occurred such as air bubbles which occasionally resulted in missed data collection points. Generally, a clear increase in H_2O_2 associated with

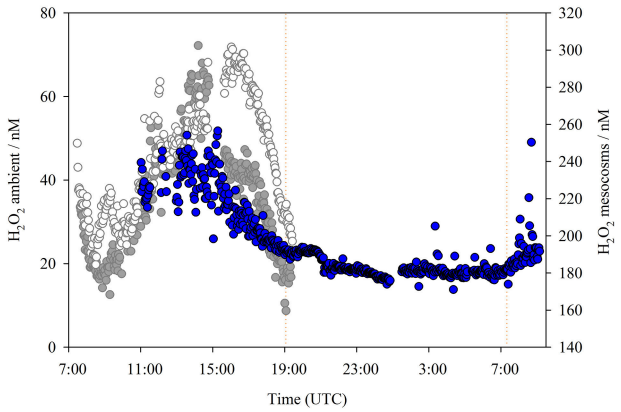

FIGURE 2 | H_2O_2 concentrations (nM) in ambient waters adjacent to the mesocosm sampling jetty over a complete diurnal cycle at ~2 min resolution (blue circles), superimposed on H_2O_2 concentrations for different days (as per **Figure 3**) from within the 1,450 µatm pCO_2 (dark gray) and 400 µatm pCO_2 (light gray) mesocosms Ambient H_2O_2 concentration data collected 5–6 March 2016. All times are UTC, sunrise/sunset (illustrated) refers to Las Palmas: sunrise (5 March) 7:21, sunset (5 March) 19:04, sunrise (6 March) 07:20. The sample line was positioned at ~10 cm depth. There was no large change in surface salinity over the experiment duration (range 0.2 practical salinity units).

daylight was evident in all three diurnal datasets (**Figures 2**, **3**). Yet H_2O_2 concentrations were much higher throughout the diurnal cycle within the mesocosms compared to ambient waters. In all three diurnal cycles, peak H_2O_2 concentration occurred mid-late afternoon (times refer to UTC). In the two mesocosms where diurnal H_2O_2 concentration was followed, the range between peak and minimum H_2O_2 was similar (180–300 nM, mesocosm 5, day 23; 160–300 nM, mesocosm 6, day 22), despite the pronounced difference in pCO_2 (400 µatm [5] compared 1,450 µatm [6]) and the 2 h offset between the timing of peak daytime H_2O_2 concentration (**Figure 3**). In ambient seawater, the amplitude of diurnal variation in H_2O_2 (~20–30 nM, **Figure 2**) was very similar to that reported previously in the central Atlantic Ocean (25 nM, Yuan and Shiller, 2001).

Two curious features were notable in both mesocosm diurnal cycles (**Figure 3**). These features could only be observed by virtue of the very high data resolution and, to some extent, also the relatively high H_2O_2 concentrations within the mesocosms compared to ambient waters. First, peak H_2O_2 concentrations occurred >1 h after peak irradiance. PAR data from ELDONET was not available for the seawater diurnal study date (**Figure 2**), but noting the timing of peak H_2O_2, there was likely approximately a 1 h offset between peak irradiance and peak H_2O_2 here also. Second, the net decline in H_2O_2 concentration which occurred in the dark continued until sometime after sunrise in both mesocosm studies (**Figure 3**). An increase in H_2O_2 was not apparent until after PAR increased above ~100 W m^{-2}. This was not apparent in the ambient seawater study (**Figure 2**) where a relatively stable concentration of 18.1 ± 1.3 nM was maintained from 21:11 to 07:20 (sunrise) with a sustained rise in H_2O_2 thereafter. This time offset could

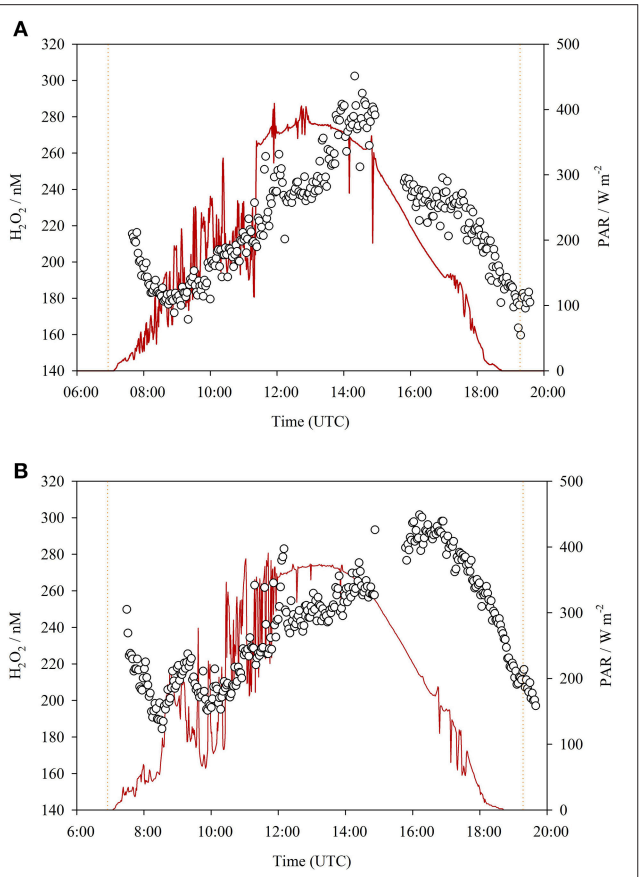

FIGURE 3 | (A) H_2O_2 measured in mesocosm 6 (1450 μatm pCO_2) surface water over a diurnal cycle (experiment day 22, 27 March 2016, sunrise 06:56, and sunset 19:17). **(B)** H_2O_2 measured in mesocosm 5 (400 μatm pCO_2) surface water over a diurnal cycle (experiment day 23, 28 March 2016, sunrise 06:55, and sunset 19:17). In both cases the sample line was positioned at ~10 cm depth. Times are UTC, sunrise/sunset refers to Las Palmas, Gran Canaria. PAR (red lines) recorded at an ELDONET site < 200 m from the mesocosm jetty.

simply therefore have related to the incident solar angle as the mesocosm walls may have reduced the rate of light induced H_2O_2 formation at low incident solar angles.

Minor H_2O_2 Additions From Rainwater

The open design of the mesocosms created the potential for significant atmospheric deposition of H_2O_2. Rain water H_2O_2 concentrations were quantified for the two rainfall events during the mesocosm experiment with sufficient amounts of deposition (>1 mm) to facilitate sampling (**Table 1**) and were similar to values reported elsewhere over the Atlantic (Zika et al., 1982; Kieber et al., 2001). H_2O_2 concentrations in rainwater are thought to be sufficiently high to offset the expected beneficial effect of rainwater derived nutrient and micro-nutrient addition on primary production when rainwater is mixed with seawater (Willey et al., 2004) unless the dilution factor is high. The calculated H_2O_2 addition to mesocosms resulting from rainfall in Gran Canaria was however modest relative to the mesocosm H_2O_2 concentrations due to the low ratio of rain:mesocosm volume (**Table 1**).

TABLE 1 | Contribution of rainwater events to H_2O_2 concentrations in the mesocosms.

Location	Date and time	Rainfall (mm)	Rainwater H_2O_2 (μM)	Calculated H_2O_2 increase in mesocosms (nM)
Taliarte, Gran Canaria	21/03/16 07:00 (day 16)	1	20.5	6
	30/03/16 17:30 (day 25)	3	44.4	40

DISCUSSION

Diurnal Cycling of H_2O_2

Photochemical processes are thought to be the dominant influence on ambient H_2O_2 concentrations in the surface ocean (O'Sullivan et al., 2005; Steigenberger and Croot, 2008), with large scale spatial variations typically explained in terms of latitudinal changes in light and ocean temperature (Yocis et al., 2000; Yuan and Shiller, 2001). In the high-resolution temporal experiments a clear diurnal cycle in H_2O_2 concentration was evident, both inside and outside the mesocosm bags (**Figures 2**, **3**). The amplitude of H_2O_2 concentration over a diurnal cycle was however much greater inside the mesocosms (100 nM compared to 20–30 nM in ambient seawater). H_2O_2 concentrations over the 28 day duration of the mesocosm experiment (**Figure 1A**) were always measured at 14:00–15:00 (UTC) daily to ensure that the month long data series was not affected unduly by diurnal variation.

During overnight monitoring of ambient H_2O_2 it appeared that an equilibrium concentration of 18 nM was maintained in the dark (**Figure 2**). This was indicative of a dark production mechanism, such as that highlighted in prior work (Palenik and Morel, 1988; Moffett and Zafiriou, 1990), sufficient to offset H_2O_2 decay. Whilst photochemical processes are no doubt a major source of H_2O_2, inter-day changes in integrated PAR were only significantly correlated with the H_2O_2 trend in ambient seawater (Spearman rank correlation 0.73, p value 0.002, $n = 14$) and in the 400 μatm mesocosm (**Table 2**). In all other mesocosms there was no apparent correlation between integrated daily PAR and H_2O_2 concentration from days 7–29.

The two high-resolution diurnal cycles within mesocosms (**Figure 3**) revealed some interesting features that would not be apparent at lower H_2O_2 concentrations (due to the increased signal:noise ratio) or reduced sampling resolution. An offset between irradiance and H_2O_2 concentration was reflected in the later delayed peak in H_2O_2 compared to maximum irradiance. Partial shading of the mesocosms in the early morning and late afternoon could create a local PAR exposure that was reduced compared to that reported by a mounted sensor. However, as the displacement of the sensor was <200 m from the mesocosms, this could not explain the offset between peak H_2O_2 and peak irradiance in the mid-afternoon. Instead, we suggest that net

TABLE 2 | Spearman rank correlation coefficients and *p* values for H_2O_2 concentration time series in each mesocosm compared to: baseline H_2O_2 concentration in ambient seawater (nM), chlorophyll a ($\mu g\ L^{-1}$), total bacteria (cells mL^{-1}), colored dissolved organic matter slope ratio (S_R), and daily integrated mean photosynthetically active radiation (PAR, W m^{-2}).

Mesocosm (number) pCO_2 (μatm)	Spearman rank correlation coefficient									
	Baseline H_2O_2			Chlorophyll a		Bacteria		CDOM SR		PAR
	Day −3 to 9	Day 11+	All days	Day 11+	All days	Day 11+	All days	Day 11+	All days	Days 7+
(5) 400	0.86	NSR	0.48	NSR	NSR	NSR	NSR	NSR	NSR	0.58
(7) 700	0.79	NSR	0.42	NSR	NSR	NSR	NSR	NSR	−0.51	NSR
(3) 850	0.81	NSR	NSR	−0.58	−0.47	−0.85	-0.52	0.70	NSR	NSR
(4) 1000	0.81	NSR	NSR	NSR	NSR	−0.87	-0.50	NSR	NSR	NSR
(8) 1150	0.86	NSR	NSR	−0.78	−0.53	−0.83	−0.56	NSR	NSR	NSR
(2) 1300	0.83	NSR	NSR	-0.61	−0.46	−0.94	−0.58	NSR	NSR	NSR
(6) 1450	0.93	NSR	NSR	NSR	NSR	−0.59	NSR	NSR	NSR	NSR
***P* VALUES**										
(5) 400	0.0018	0.44	0.019	0.29	0.87	0.15	0.59	0.92	0.50	0.028
(7) 700	0.015	0.23	0.040	0.74	0.91	0.081	0.16	0.85	0.035	0.13
(3) 850	0.0096	0.76	0.33	0.035	0.030	<0.001	0.023	0.010	0.17	0.66
(4) 1000	0.0096	0.82	0.12	0.098	0.36	<0.001	0.028	0.97	0.99	0.20
(8) 1150	0.0018	0.67	0.57	<0.001	0.013	<0.001	0.013	0.72	0.54	0.92
(2) 1300	0.0053	0.73	0.38	0.025	0.034	<0.001	0.010	0.60	0.54	0.70
(6) 1450	<0.001	0.70	0.46	0.17	0.60	0.031	0.28	0.85	0.20	0.22

NSR, no significant relationship ($P > 0.05$). Highly significant correlations (P 0.010 or less) are highlighted. Mesocosm 1 (550 μatm pCO_2), was excluded due to the lack of data after day 3.

biological production of H_2O_2 is slightly offset from irradiance. A critical factor, not measured herein, which likely affects the net rate of change in H_2O_2 concentration during daylight hours is the production rate of peroxidase or catalase enzymes. This process is known to be diurnally variable, with oxidative defenses more active during daylight hours (Morris et al., 2016). Whilst it is not clear if this response under natural conditions is triggered by increasing H_2O_2 induced stress or by a circadian rhythm, the rate and efficiency (which may also change with incident light) of enzymatic H_2O_2 removal are likely to be key influences on the shape of the diurnal H_2O_2 trend.

Correlation of H_2O_2 in Mesocosms With Core Parameters

Between days −3 and 9 the range of H_2O_2 within the different mesocosms was small (<45 nM) and the behavior of chlorophyll a and nitrate very similar across all mesocosms (**Figures 1A–C**). During this early phase, H_2O_2 inside and outside the mesocosms was relatively well correlated across all pCO_2 conditions (positive Spearman Rank Coefficients of 0.79–0.93). Combined with the comparability of the diurnal H_2O_2 cycle in 400 and 1,450 µatm pCO_2 mesocosms (**Figure 3**), despite the extreme pCO_2 difference, this suggests that the direct effect of the pCO_2 gradient (applied after day 0) on H_2O_2 concentrations was minimal.

In contrast to the early stage of the experiment, H_2O_2 concentrations in the mesocosms diverged after day 9 and there was then no longer a statistically significant relationship between the paired H_2O_2 concentrations in and outside the mesocosm (Spearman Rank Correlation $P > 0.05$, **Table 2**) for any pCO_2 treatment. If irradiance was the dominant factor controlling extracellular H_2O_2 concentrations throughout the experiment, we would expect H_2O_2 concentrations to have remained similar across all mesocosms and to remain correlated with H_2O_2 in ambient water outside the mesocosms. Yet this was not the case. Variations in daily integrated PAR, available from day 7 onwards, could explain some of the variation in background seawater H_2O_2, but inter-day changes in PAR were only significantly correlated with H_2O_2 in the 400 µatm mesocosm (**Table 2**).

Formation of ROS generally increases with dissolved organic carbon concentration in estuarine waters and this is specifically linked to the presence of terrestrially derived humic material (Timko et al., 2014) which has a relatively large component of CDOM. However, CDOM properties are not clearly linked to increasing H_2O_2 concentrations in offshore seawater (O'Sullivan et al., 2005). The general decline in S_R throughout the mesocosms (from day 1 to day 27, **Figure 1E**) suggested that *in situ* production of higher molecular weight CDOM was sufficient to offset photo bleaching. However, this was not clearly related to any change in H_2O_2 concentration as no clear correlation was found between S_R and H_2O_2 either over the whole experiment or specifically for days 11+ (**Table 2**).

Similarly, the overall trend in H_2O_2 concentration could not be related directly to macronutrient depletion. The observed nitrate concentrations were similar across all mesocosms until after the addition of macronutrients on day 18 (**Figure 3**) and there was no consistent trend in H_2O_2 concentration in the days immediately following this addition. Most mesocosms obtained the highest measured H_2O_2 concentration between days 9–18. Yet mesocosm 6 was notable for obtaining a peak H_2O_2

concentration 3 days after the nutrient addition. A sustained drop in H_2O_2 concentration across all mesocosms (apart from the anomalous mesocosm 7) was only observed between days 23–25.The lowest H_2O_2 concentrations, both within the mesocosm experiment and relative to ambient seawater, were observed in this post-bloom phase when bacterial abundance peaked (**Figure 1D**) and when daily integrated PAR was persistently low for 3 days (**Figure 1F**).

A Contribution to H_2O_2 From Mesocosm Design?

H_2O_2 concentrations might be expected to be generally higher inside the mesocosms due to the nature of their design. Sunlight is attenuated with depth, so in a natural surface mixed layer H_2O_2 is formed predominantly at the surface and then physically mixed throughout the surface mixed layer (Johnson et al., 1989; Miller and Kester, 1994), although sub-surface H_2O_2 peaks can occasionally be observed at the chlorophyll a maxima (Yuan and Shiller, 2001; Croot et al., 2005; Steigenberger and Croot, 2008) . The confinement of the surface 3 m within the mesocosm bags used here thereby encloses the water with the highest light exposure and, throughout most of this experiment, a high level of biological activity relative to ambient seawater, whilst removing the physical processes that would constantly act to mix H_2O_2 into deeper waters. The enclosure of seawater was thereby a likely factor contributing to the high H_2O_2 concentrations occurring during the middle (days 9–18) of the mesocosm experiment. Yet this alone does not explain the divergence in H_2O_2 levels between the various mesocosms after day 9 (**Figure 1A**). The timings of the initial mini-bloom after the mesocosms were filled, of the macronutrient addition and the subsequent bloom were (with the exception of mesocosm 7) relatively uniform (**Figures 1B,C**).

A Link Between Community Structure and Extracellular H_2O_2?

Two possible explanations for why H_2O_2 concentrations were so variable between mesocosms, which are not mutually exclusive, are that either the biological H_2O_2 source(s) or the biological H_2O_2 sink(s) varied because of different microbial communities across the pCO_2 gradient. An anti-correlation between bacterial abundance and extracellular H_2O_2 concentrations is therefore intriguing. Microorganisms are simultaneously both a H_2O_2 source and a H_2O_2 sink. ROS are generated as waste products from aerobic cellular metabolism (Kruk, 1998; Apel and Hirt, 2004), with H_2O_2 produced both directly and from the decay of other ROS (for example, the enzyme superoxide dismutase produces H_2O_2 from O_2^-; McCord and Fridovich, 1969). Conversely, biological H_2O_2 sinks arise from both synthesis of H_2O_2 destroying enzymes (catalase and peroxidase) and also, under some circumstances, serendipitously with increasing biomass. The quenching of extracellular H_2O_2 with increasing biomass is referred to as "self-shading" and has been described both in monocultures of *Prochlorococcus*, which lacks catalase-peroxidase genes (Morris et al., 2011) and at the community level (Barros and Colepicolo, 2003). It presumably arises from physical shading and/or non-enzymatic ROS sinks.

The anti-correlation between H_2O_2 concentrations in each mesocosm both with chlorophyll a and with total bacterial abundance over the duration of the experiment (**Table 2**) was statistically significant in most mesocosms. Overall there was a significant ($P < 0.05$) anti-correlation between chlorophyll a and H_2O_2 concentrations with negative correlation coefficients (**Table 2**) in mesocosms 3, 4, 8, and 2 (850–1,300 μatm pCO_2). The anti-correlation was slightly stronger when the initial phase of the experiment (Days −3 to 9, when the range of H_2O_2 concentrations across all mesocosms was relatively narrow) was excluded. A negative relationship between chlorophyll a and H_2O_2 concentrations could arise from an increasing biological H_2O_2 sink simply due to self-shading associated with increasing biomass, yet no correlation with chlorophyll a was found either at low (400, 700 μatm) or at the highest (1,450 μatm) pCO_2 treatments. For bacteria, the correlation followed the same pattern as chlorophyll a with respect to pCO_2, yet the effect was stronger and more significant. From day 11 onwards, the intermediate pCO_2 mesocosms (850–1,300 μatm) all exhibited a strong negative correlation (Spearman Rank Coefficients of −0.83 to −0.94) between bacteria cell counts and H_2O_2 concentration (P values < 0.001). This suggests that under post-bloom conditions, bacteria were an important net-sink for extracellular H_2O_2.

As both cellular H_2O_2 production and defense mechanism activity vary over diurnal cycles and at the species level, it is difficult to separate the source and sink terms within separate mesocosms and over the pCO_2 gradient. Yet in any case, the effects of a pCO_2 gradient on H_2O_2 concentration were apparently indirect, resulting from changes to bacterial abundance and community composition rather than directly arising as a consequence of perturbing the carbonate system alone.

Effects of Elevated H_2O_2 Under Experimental Conditions?

Reported H_2O_2 concentrations in seawater incubated under laboratory conditions are typically 100–300 nM (e.g., Coe et al., 2016), but can be much higher depending on the buffer composition and irradiance exposure (Morris and Zinser, 2013). In a spot-check of baseline H_2O_2 concentrations in incubated seawater (with added nutrients) in our own laboratory, we found 42 ± 50 nM H_2O_2 in freshly made mixtures (made from seawater which was previously stored in the dark for >1 year) and 180 ± 130 nM in the same water after 72 h of incubation subject to a diel light cycle. In all these cases, the H_2O_2 concentrations in seawater incubated under laboratory conditions are thereby at the mid-high end of the range observed in the surface ocean (Price et al., 1998; Yuan and Shiller, 2001; Hopwood et al., 2017).

The unmodified concentrations of H_2O_2 in growth media are sufficiently high to prevent the cultivation of some microorganisms, including strains of *Prochlorococcus*, under laboratory conditions (Morris et al., 2011). However, uncertainties remain about what the effects of elevated H_2O_2 are

at the community level. Whilst H_2O_2 is not widely investigated during mesocosm studies, field evidence suggests that increases in H_2O_2 to concentrations less than the peaks observed here (**Figure 1A**) can affect a broad range of biogeochemical processes. Additions of 10–100 nM H_2O_2 to water from 100 m in the North Atlantic were found to reduce the extracellular activity of β-glucosidase, alkaline phosphatase, and leucine aminopeptidase by 20–80% with the inhibition effect consistently strongest on β-glucosidase (Baltar et al., 2013). A similar small absolute increase of only 30 nM is reported to suppress rates of ammonia oxidation to below detection in surface (10 m depth) Antarctic seawater (Tolar et al., 2016) where the initial natural concentration of H_2O_2 was low (14 nM). Additional specific effects of increasing extracellular H_2O_2 concentrations in seawater can also be deduced from laboratory experiments. For example, an increase on the order of 100 nM H_2O_2 is sufficient to measurably decrease the half-life of Fe(II), thereby theoretically decreasing dissolved Fe bioavailability (González-Davila et al., 2005), and to double brominating activity in some diatoms (Hughes and Sun, 2016).

A particularly curious phenomenon observed here was the extremely high H_2O_2 concentrations observed during the pre-bloom phase of the experiment (**Figure 1A**). It is questionable to what extent this phenomenon would occur in a natural environment because small-scale mesocosms inevitably fail to mimic the mixing processes that occur within the natural water column. Nevertheless, the potential for oxidative stress from extracellular ROS to be increased under natural, or incubated, oligotrophic conditions should be investigated concurrently with other stressors to understand the interactive effect(s) on microbial functioning. As outlined above, the sensitivity of some enzymatic processes to increasing extracellular H_2O_2 concentrations and the involvement of H_2O_2 in the biogeochemical cycling of various chemicals including the micronutrient Fe, means that large perturbations to H_2O_2 during mesocosm experiments are undesirable.

CONCLUSIONS

During the progression of a 28 day mesocosm experiment in North Atlantic waters an applied pCO_2 gradient (400–1,450 μatm) had no discernable direct effect upon extracellular H_2O_2 concentrations. Whilst a clear diurnal trend in H_2O_2 was observed, both within high/low pCO_2 mesocosms and in ambient waters, inter-day variation in PAR was not correlated with mesocosm H_2O_2 concentrations.

The general elevation of H_2O_2 above ambient North Atlantic concentrations was attributed to the effect of enclosing seawater in an open mesocosm at the ocean surface. Yet during the pre-bloom phase of the experiment, unexpected swings occurred to H_2O_2 concentrations >300 nM. Across the majority of mesocosms, bacteria appeared to be a net-sink for H_2O_2, particularly under post-bloom conditions. Thus, microbial community structure does appear to strongly influence extracellular H_2O_2 concentrations.

Given the multitude of possible direct and indirect, chemical and biological effects of large changes to H_2O_2 concentrations, it is important to consider to what extent ROS are a source of oxidative stress in the natural surface ocean and how well experiments manipulate the natural environment with respect to this stressor.

AUTHOR CONTRIBUTIONS

All authors contributed to the design of the study. Fieldwork and analytical work was conducted by MH, UR, AL, JA, and NH. MH wrote the initial draft of the manuscript and then all authors contributed to its revision.

FUNDING

Funding for this mesocosm study was provided by the Kiel Excellence Cluster The Future Ocean and by the German Research Foundation (DFG) through the Leibniz Award 2012 to UR. MH and EA gratefully acknowledge financial aid from the European Commission (OCEAN-CERTAIN, FP7-ENV-2013-6.1-1; no: 603773) and the Collaborative Research Centre 754 (SFB 754) Climate-Biogeochemistry Interactions in the Tropical Ocean funded by the German Research Foundation (DFG). JA was supported by a Helmholtz International Fellow Award, 2015 (Helmholtz Association, Germany). NH was partially supported by the FLUXES project (CTM2015-69392-C3-1-R) funded by the Spanish government (Plan Nacional I+D).

ACKNOWLEDGMENTS

The KOSMOS/PLOCAN teams assisting with all aspects of mesocosm organization are thanked for logistical support. Leila Kittu and Syrmalenia Kotronaki are thanked for chlorophyll a and macronutrient data. Labview software for operating the H_2O_2 FIA system was designed by P. Croot, M. Heller, C. Neill, and W. King. Statistics were performed in SigmaPlot.

SUPPLEMENTARY MATERIAL

The Supplementary Material for this article can be found online at: https://www.frontiersin.org/articles/10.3389/fmars.2018.00105/full#supplementary-material

Supplementary Figure 1 | Mesocosm timeline labeled with experiment days (used throughout the text). Day −4, when the mesocosms were filled, was 1 March 2016. A pH gradient was imposed on day 0 by the addition of CO_2 saturated, filtered seawater. Further pCO_2 additions were then made as necessary to compensate for out-gassing. The volume of each mesocosm was determined on day 18 by measuring the change in salinity resulting from a freshwater addition. A single macronutrient spike was then added after sampling on day 18.

Supplementary Datasheet 1 | Mesocosm time series data for core parameters used: chlorophyll a, nitrate + nitrite, hydrogen peroxide, bacterial abundance and CDOM SR.

REFERENCES

Apel, K., and Hirt, H. (2004). Reactive oxygen species: metabolism, oxidative stress, and signal transduction. *Annu. Rev. Plant Biol.* 55, 373–399. doi: 10.1146/annurev.arplant.55.031903.141701

Baltar, F., Reinthaler, T., Herndl, G. J., and Pinhassi, J. (2013). Major effect of hydrogen peroxide on bacterioplankton metabolism in the Northeast Atlantic. *PLoS ONE* 8:e61051. doi: 10.1371/journal.pone.0061051

Barros, M. P., and Colepicolo, P. (2003). Self-shading protects phytoplankton communities against H_2O_2-induced oxidative damage. *Aquat. Microb. Ecol.* 30, 275–282. doi: 10.3354/ame030275

Bogosian, G., Aardema, N. D., Bourneuf, E. V., Morris, P. J. L., and O'Neil, J. P. (2000). Recovery of hydrogen peroxide-sensitive culturable cells of *Vibrio vulnificus* gives the appearance of resuscitation from a viable but nonculturable state. *J. Bacteriol.* 182, 5070–5075. doi: 10.1128/JB.182.18.5070-5075.2000

Coe, A., Ghizzoni, J., LeGault, K., Biller, S., Roggensack, S. E., and Chisholm, S. W. (2016). Survival of Prochlorococcus in extended darkness. *Limnol. Oceanogr.* 61, 1375–1388. doi: 10.1002/lno.10302

Croot, P. L., Laan, P., Nishioka, J., Strass, V., Cisewski, B., Boye, M., et al. (2005). Spatial and temporal distribution of Fe(II) and H_2O_2 during EisenEx, an open ocean mescoscale iron enrichment. *Mar. Chem.* 95, 65–88. doi: 10.1016/j.marchem.2004.06.041

Croot, P. L., Streu, P., Peeken, I., Lochte, K., and Baker, A. R. (2004). Influence of the ITCZ on H2O2 in near surface waters in the equatorial Atlantic Ocean. *Geophys. Res. Lett.* 31:L23S04. doi: 10.1029/2004GL020154

Czerny, J., Schulz, K. G., Krug, S. A., Ludwig, A., and Riebesell, U. (2013). Technical note: the determination of enclosed water volume in large flexible-wall mesocosms KOSMOS. *Biogeosciences* 10, 1937–1941. doi: 10.5194/bg-10-1937-2013

Fujiwara, K., Ushiroda, T., Takeda, K., Kumamoto, Y., and Tsubota, H. (1993). Diurnal and seasonal distribution of hydrogen-peroxide in seawater of the seto inland sea. *Geochem. J.* 27, 103–115. doi: 10.2343/geochemj.27.103

Gasol, J. M., and del Giorgio, P. A. (2000). Using flow cytomery for counting natural planktonic bacteria and understanding the structure of planktonic bacterial communities. *Sci. Mar.* 64, 197–224. doi: 10.3989/scimar.2000.64n2197

Gerringa, L. J. A., Rijkenberg, M. J. A., Timmermans, R., and Buma, A. G. J. (2004). The influence of solar ultraviolet radiation on the photochemical production of H_2O_2 in the equatorial Atlantic Ocean. *J. Sea Res.* 51, 3–10. doi: 10.1016/j.seares.2003.03.002

González-Davila, M., Santana-Casiano, J. M., and Millero, F. J. (2005). Oxidation of iron (II) nanomolar with H_2O_2 in seawater. *Geochim. Cosmochim. Acta* 69, 83–93. doi: 10.1016/j.gca.2004.05.043

Häder, D.-P., and Lebert, M. (2006). "Eldonet—European light dosimeter network BT - environmental UV radiation: impact on ecosystems and human health and predictive models," in *Proceedings of the NATO Advanced Study Institute on Environmental UV Radiation: Impact on Ecosystems and Human Health*, eds F. Ghetti, G. Checcucci, and J. F. Bornman (Dordrecht: Springer Netherlands), 95–108.

Hansen, H. P., and Koroleff, F. (1999). "Determination of nutrients," in *Methods of Seawater Analysis*, eds K. Grasshoff, K. Kremling, and M. Ehrhardt (New York, NY: Wiley-VCH Verlag GmbH), 159–228.

Helms, J. R., Stubbins, A., Ritchie, J. D., Minor, E. C., Kieber, D. J., and Mopper, K. (2008). Absorption spectral slopes and slope ratios as indicators of molecular weight, source, and photobleaching of chromophoric dissolved organic matter. *Limonol. Oceanogr.* 53, 955–969. doi: 10.4319/lo.2008.53.3.0955

Hopwood, M. J., Rapp, I., Schlosser, C., and Achterberg, E. P. (2017). Hydrogen peroxide in deep waters from the Mediterranean Sea, South Atlantic and South Pacific Oceans. *Sci. Rep.* 7:43436. doi: 10.1038/srep43436

Hughes, C., and Sun, S. (2016). Light and brominating activity in two species of marine diatom. *Mar. Chem.* 181, 1–9. doi: 10.1016/j.marchem.2016.02.003

Imlay, J. A. (2008). Cellular defenses against superoxide and hydrogen peroxide. *Annu. Rev. Biochem.* 77, 755–776. doi: 10.1146/annurev.biochem.77.061606.161055

IPCC Working Group 1 (2014). *IPCC Fifth Assessment Report (AR5) - The Physical Science Basis*. IPCC Working Group.

Johnson, K. S., Willason, S. W., Wiesenburg, D. A., Lohrenz, S. E., and Arnone, R. A. (1989). Hydrogen peroxide in the western Mediterranean Sea: a tracer for vertical advection. *Deep Sea Res. Oceanogr. Res. Pap.* 36, 241–254. doi: 10.1016/0198-0149(89)90136-2

Kieber, R. J., Peake, B., Willey, J. D., and Jacobs, B. (2001). Iron speciation and hydrogen peroxide concentrations in New Zealand rainwater. *Atmos. Environ.* 35, 6041–6048. doi: 10.1016/S1352-2310(01)00199-6

Kruk, I. (1998). *Environmental Toxicology and Chemistry of Oxygen Species*, *1st Edn*. Berlin; Heidelberg: Springer-Verlag.

Lesser, M. P. (2006). Oxidative stress in marine environments: biochemistry and physiological ecology. *Annu. Rev. Physiol.* 68, 253–278. doi: 10.1146/annurev.physiol.68.040104.110001

McCord, J. M., and Fridovich, I. (1969). Superoxide dismutase. An enzymic function for erythrocuprein (hemocuprein). *J. Biol. Chem.* 244, 6049–6055.

Micinski, E., Ball, L. A., and Zafiriou, O. C. (1993). Photochemical oxygen activation: superoxide radical detection and production rates in the eastern Caribbean. *J. Geophys. Res. Ocean.* 98, 2299–2306. doi: 10.1029/92JC02766

Miller, W. L., and Kester, D. R. (1994). Peroxide variations in the Sargasso Sea. *Mar. Chem.* 48, 17–29. doi: 10.1016/0304-4203(94)90059-0

Milne, A., Davey, M. S., Worsfold, P. J., Achterberg, E. P., and Taylor, A. R. (2009). Real-time detection of reactive oxygen species generation by marine phytoplankton using flow injection-chemiluminescence. *Limnol. Oceanogr.* 7, 706–715. doi: 10.4319/lom.2009.7.706

Moffett, J. W., and Zafiriou, O. C. (1990). An investigation of hydrogen peroxide chemistry in surface waters of Vineyard Sound with $H_2^{18}O_2$ and $^{18}O_2$. *Limnol. Oceanogr.* 35, 1221–1229. doi: 10.4319/lo.1990.35.6.1221

Moore, C. A., Farmer, C. T., and Zika, R. G. (1993). Influence of the Orinoco River on hydrogen peroxide distribution and production in the eastern Caribbean. *J. Geophys. Res.* 98:2289. doi: 10.1029/92JC02767

Morris, J. J., Johnson, Z. I., Szul, M. J., Keller, M., and Zinser, E. R. (2011). Dependence of the cyanobacterium Prochlorococcus on hydrogen peroxide scavenging microbes for growth at the ocean's surface. *PLoS ONE* 6:e16805. doi: 10.1371/journal.pone.0016805

Morris, J. J., Johnson, Z. I., Wilhelm, S. W., and Zinser, E. R. (2016). Diel regulation of hydrogen peroxide defenses by open ocean microbial communities. *J. Plankton Res.* 38, 1103–1114. doi: 10.1093/plankt/fbw016

Morris, J. J., Kirkegaard, R., Szul, M. J., Johnson, Z. I., and Zinser, E. R. (2008). Facilitation of robust growth of Prochlorococcus colonies and dilute liquid cultures by "helper" heterotrophic bacteria. *Appl. Environ. Microbiol.* 74, 4530–4534. doi: 10.1128/AEM.02479-07

Morris, J., and Zinser, E. R. (2013). Continuous hydrogen peroxide production by organic buffers in phytoplankton culture media. *J. Phycol.* 49, 1223–1228. doi: 10.1111/jpy.12123

O'Sullivan, D. W., Neale, P. J., Coffin, R. B., Boyd, T. J., and Osburn, C. L. (2005). Photochemical production of hydrogen peroxide and methylhydroperoxide in coastal waters. *Mar. Chem.* 97, 14–33. doi: 10.1016/j.marchem.2005.04.003

Palenik, B., and Morel, F. M. M. (1988). Dark production of H_2O_2 in the Sargasso Sea. *Limnol. Oceanogr.* 33, 1606–1611. doi: 10.4319/lo.1988.33.6_part_2.1606

Palenik, B., Zafiriou, O. C., and Morel, F. M. M. (1987). Hydrogen peroxide production by a marine phytoplankter. *Limnol. Oceanogr.* 32, 1365–1369. doi: 10.4319/lo.1987.32.6.1365

Petasne, R. G., and Zika, R. G. (1997). Hydrogen peroxide lifetimes in South Florida coastal and offshore waters. *Mar. Chem.* 56, 215–225. doi: 10.1016/S0304-4203(96)00072-2

Price, D., Mantoura, R. F. C., and Worsfold, P. J. (1998). Shipboard determination of hydrogen peroxide in the western Mediterranean sea using flow injection with chemiluminescence detection. *Anal. Chim. Acta* 377, 145–155. doi: 10.1016/S0003-2670(98)00621-7

Riebesell, U., Czerny, J., Von Bröckel, K., Boxhammer, T., Büdenbender, J., Deckelnick, M., et al. (2013). Technical note: a mobile sea-going mesocosm system - new opportunities for ocean change research. *Biogeosciences* 10, 1835–1847. doi: 10.5194/bg-10-1835-2013

Seaver, L. C., and Imlay, J. A. (2001). Hydrogen peroxide fluxes and compartmentalization inside growing *Escherichia coli*. *J. Bacteriol.* 183, 7182–7189. doi: 10.1128/JB.183.24.7182-7189.2001

Steigenberger, S., and Croot, P. L. (2008). Identifying the processes controlling the distribution of H_2O_2 in surface waters along a meridional transect in the eastern Atlantic. *Geophys. Res. Lett.* 35:L03616. doi: 10.1029/2007GL032555

Taucher, J. (2017). Influence of ocean acidification and deep water upwelling on oligotrophic plankton communities in the subtropical North

Atlantic: insights from an *in situ* Mesocosm study. *Front. Mar. Sci.* 4:85. doi: 10.3389/fmars.2017.00085

Timko, S. A., Romera-Castillo, C., Jaffé, R., and Cooper, W. J. (2014). Photoreactivity of natural dissolved organic matter from fresh to marine waters in the Florida Everglades, USA. *Environ. Sci. Process. Impacts* 16, 866–878. doi: 10.1039/C3EM00591G

Tolar, B., Powers, L., Miller, W., Wallsgrove, N., Popp, B., and Hollibaugh, J. (2016). Ammonia oxidation in the ocean can be inhibited by nanomolar concentrations of hydrogen peroxide. *Front. Mar. Sci.* 3:237. doi: 10.3389/fmars.2016.00237

Van Baalen, C., and Marler, J. E. (1966). Occurrence of hydrogen peroxide in sea water. *Nature* 211:951. doi: 10.1038/211951a0

Vermilyea, A. W., Hansard, S. P., and Voelker, B. M. (2010). Dark production of hydrogen peroxide in the Gulf of Alaska. *Limnol. Oceanogr.* 55, 580–588. doi: 10.4319/lo.2009.55.2.0580

Welschmeyer, N. A. (1994). Fluorometric analysis of chlorophyll a in the presence of chlorophyll b and pheopigments. *Limnol. Oceanogr.* 39, 1985–1992. doi: 10.4319/lo.1994.39.8.1985

Willey, J. D., Kieber, R. J., and Avery, G. B. (2004). Effects of rainwater iron and hydrogen peroxide on iron speciation and phytoplankton growth in seawater near Bermuda. *J. Atmos. Chem.* 47, 209–222. doi: 10.1023/B:JOCH.0000021087.19846.e1

Yocis, B. H., Kieber, D. J., and Mopper, K. (2000). Photochemical production of hydrogen peroxide in Antarctic Waters. *Deep. Res. I* 47, 1077–1099. doi: 10.1016/S0967-0637(99)00095-3

Yuan, J. C., and Shiller, A. M. (1999). Determination of subnanomolar levels of hydrogen peroxide in seawater by reagent-injection chemiluminescence detection. *Anal. Chem.* 71, 1975–1980. doi: 10.1021/ac981357c

Yuan, J., and Shiller, A. (2001). The distribution of hydrogen peroxide in the southern and central Atlantic ocean. *Deep Sea Res. II Top. Stud. Oceanogr.* 48, 2947–2970. doi: 10.1016/S0967-0645(01)00026-1

Yuan, J., and Shiller, A. M. (2004). Hydrogen peroxide in deep waters of the North Pacific Ocean. *Geophys. Res. Lett.* 31:L01310. doi: 10.1029/2003GL018439

Zika, R., Saltzman, E., Chameides, W. L., and Davis, D. D. (1982). H_2O_2 levels in rainwater collected in south Florida and the Bahama Islands. *J. Geophys. Res.* 87:5015. doi: 10.1029/JC087iC07p05015

Conflict of Interest Statement: The authors declare that the research was conducted in the absence of any commercial or financial relationships that could be construed as a potential conflict of interest.